Dynamics of Atmospheres and Oceans, 7 (1983) 189–219
Elsevier Science Publishers B.V., Amsterdam – Printed in The Netherlands

EIKONAL DESCRIPTION OF INTERNAL WAVE INTERACTIONS: A NON-DIFFUSIVE PICTURE OF "INDUCED DIFFUSION"

FRANK S. HENYEY and NEIL POMPHREY

Center for Studies of Nonlinear Dynamics, La Jolla Institute, P.O. Box 1434, La Jolla, CA 92038 (U.S.A.)

(Received July 14, 1982; revised April 15, 1983; accepted May 20, 1983)

ABSTRACT

Henyey, F.S. and Pomphrey, N., 1983. Eikonal description of internal wave interactions: a non-diffusive picture of "induced diffusion". Dyn. Atmos. Oceans, 7: 189–219.

We use eikonal theory to investigate the "induced diffusion" interaction in the ocean between small-scale internal waves and a much larger scale internal wave field. Surprising results are found. The eikonal description follows transport in both position and wavenumber space. The approach consists of modeling the small-scale portion as a superposition of wave packets, each of which moves through the large-scale flow according to the laws of particle mechanics: trajectories are determined by the solution of Hamilton's ordinary differential equations of motion, with a Hamiltonian given by a dispersion relation $H(\mathbf{k}, \mathbf{x}) = \omega = \sigma(\mathbf{k}) + \mathbf{v}_0 \cdot \mathbf{k}$. The first term on the right-hand side is the dispersion relation in the absence of the large-scale flow, $\mathbf{v}_0$, and the second term is a Doppler shift that describes the interaction between the different scales. We give a careful derivation of the eikonal equations for a fluid, starting with a Hamiltonian description of the fluid flow (Section 2). A discussion is given of the important difference in meaning between the total energy of the wave packet, ωA, and the intrinsic energy, σA (A is the action). We also clarify the existence of a Stokes drift for internal waves (Section 3). Numerical experiments were performed which consist of following the motion of the center of a wave packet as it propagates through a Garrett–Munk field of internal waves (Section 4). The initial conditions of the packet were chosen to lie within the induced diffusion kinematic regime. A total of 50 trajectories were obtained from which average properties were calculated. The results of our numerical experiments show that horizontal transport is unimportant, whereas transport through vertical wavenumbers is very significant. We find a mean motion of k_v to large values with the same sign as at $t = 0$, and fluctuations about that mean. The individual excursions in $k_v(t)$ are of large magnitude, and we argue that the traditional idea of diffusion in $k_v - t$ space, implying a random walk, is inappropriate. Thirtyfour out of the 50 trajectories in our sample reached a vertical wavelength cut-off placed at 5 m, doing so in essentially the same way as trajectories which approach a critical layer in a time and horizontal position independent shear flow. On the basis of our numerical results we provide a simple model which describes much of the transport that occurs. We argue that diffusion occurs in $\sigma - z$ space, and a simple "mean first passage" calculation allows us to derive an expression for the probability density of critical layers.

0377-0265/83/$03.00

1. INTRODUCTION

The subject of this paper is an eikonal investigation of the interaction of small-scale internal waves with a much larger scale internal wave field.

Observational data suggests a "universal" steady state velocity spectrum for oceanic internal waves (Garrett and Munk, 1979). Several papers have attempted to understand the role of wave–wave interaction in determining the observed spectral shape (Olbers, 1976; McComas, 1977; McComas and Bretherton, 1977; Pomphrey et al., 1980; McComas and Muller, 1981). Common to all of these attempts has been the description of wave interactions in terms of normal modes of the linear equations of fluid motion. The earliest detailed calculations assumed that the internal wave field is weakly turbulent, and representable as a statistical ensemble of weakly coupled wave modes. In this case the Hasselman transport theory (Hasselman, 1962) is valid, which provides an evolution equation for action density in wavenumber space ensemble averaged over realizations of the chosen wave field. The work of McComas and Bretherton (1977) was particularly important here. Using the Garrett–Munk spectrum to represent the internal wave field, these authors presented a simplified picture of action transfer in terms of three "limiting triad mechanisms". One of these mechanisms, named induced diffusion, is particularly significant since it accounts for most of the action transport at high frequencies ($\sigma \gtrsim 5f$, $f \equiv$ Coriolis frequency) and modenumbers ($m \gtrsim 10$). Transport rates, however, are too high to believe the weak interaction theory which is used to calculate the rates (Holloway, 1982).

The physical description of induced diffusion as the interaction between small-scale, high-frequency internal waves ("test" waves) and a much larger scale, low-frequency flow suggests a relationship with the Taylor–Goldstein equation which is used to discuss the stability of stratified shear flows. Meiss and Watson (1982) have recently exploited this relationship to derive relaxation rates for internal waves in the induced diffusion domain, without the need to make any weak interaction assumption (their analysis is based on a *linear* equation). In order to sum all orders of perturbation theory, however, it was crucial for Meiss and Watson to require that

$$P_l(t) = h_l^2\left(\mathbf{K} \pm \frac{\mathbf{l}}{2}, \mathbf{K} \pm \frac{\mathbf{l}}{2}\right)\left[C_l^*(t)e^{i\Delta_- t} + C_l(t)e^{i\Delta_+ t}\right]\langle |c_l|^2\rangle$$

be independent of the average wavenumber, K, of the incoming and outgoing test waves, over an interval of time for which the interaction with the background must be handled deterministically. This time is the correlation time of the background as viewed by the system of small-scale waves. In this expression, $\langle |c_l|^2\rangle$ and C_l are the intensity and autocorrelation function of

the background which, by definition, are independent of K. Meiss and Watson demonstrate that the mode coupling coefficient, h_l, is very nearly independent of K. This leaves only the frequency mismatches

$$\Delta_{\pm} = \sigma_{K+l/2} - \sigma_{K-l/2} \pm \sigma_l$$

which can depend on K. Since $l \ll K$ for induced diffusion, Δ can be expanded as

$$\Delta_{\pm} = \mathbf{l} \cdot \left(\mathbf{v}_{\text{group}}(K) \pm \mathbf{v}_{\text{phase}}(l) \right)$$

The neglect of the K dependence in $\Delta_{\pm}$ amounts to the assumption that, over the correlation time, the group velocities of the short waves do not respond to the background. It follows that the position of a wave packet, $\int \mathbf{v}_{\text{group}} dt + \mathbf{x}_0$, is uncorrelated with any property of the background, given this approximation. Meiss and Watson calculate relaxation rates for short waves which are substantially reduced from those predicted by weak interaction theory, being within a factor of 10 of the linear frequency even at the highest modenumbers. Nevertheless, the picture of induced diffusion as providing the significant transport mechanism for internal waves remained intact.

In the approaches described so far, the mode amplitude is the fundamental quantity whose time evolution is followed. Unless one is able to follow the phases of these modes extremely well, and in particular to determine correctly subtle phase correlations between modes, position space information is incorrectly described. Yet position space information can be important in understanding the processes involved and in assessing the validity of approximations, and can be interesting in itself in comparison with observations on position space transport and in connection with sources and sinks of energy.

The eikonal description, in contrast to the mode description, follows transport in both position and wavenumber space. The fundamental object in this description is the Wigner function, with the uncertainty constraint (that the position of a wave cannot be defined to better than about a half wavelength) usually ignored (correction methods, however, are available; see Henyey (1980)). The Wigner function is the analog for waves of the simultaneous specification of the position and velocity of a molecule in a fluid. The Boltzmann equation for molecules follows transport in both position and velocity. We have performed, and will present in this paper, a detailed numerical investigation of transport in the "induced diffusion" kinematic regime using eikonal theory. We will present numerical evidence and a plausibility argument that the vertical position of a wave packet is strongly correlated with the background, and that this correlation is a dominant effect in the evolution of the vertical wavenumber.

The transport of action through vertical wavenumber space is therefore

sensitive to the vertical position dependence of the action. If we were to assume that the vertical group velocity of a wave packet remains constant over a background correlation time, then the vertical wavenumber transport would look very different. This case would correspond to a different representation of the same set of approximations made by Meiss and Watson, and we would expect our calculation of the evolution of the Wigner function to agree with that of Meiss and Watson. In the absence of our making such an approximation, however, we expect that the two sets of results are different.

The eikonal approach is valid in cases where there is a scale separation, such as there is for induced diffusion. The approach consists of imagining the small-scale wave field as a collection of "molecules", each with a position and wavenumber. These "molecules" are not to be thought of as isolated objects with rigid boundaries, but generally overlap one another, and fill all of the available space. The actual wave field is then the superposition of all the wave packets associated with all the molecules. Each wave packet moves along a definite trajectory, much as a particle moves along its path. The trajectories are determined by a Hamiltonian given by the dispersion relation, $\omega = H(\mathbf{k}, \mathbf{x})$, entirely analogous to classical mechanics where $E = H(\mathbf{p}, \mathbf{x})$ determines the trajectory of a particle. Hamilton's equations are $\mathbf{v} = \partial\omega/\partial\mathbf{k}$, the group velocity, and $\mathrm{d}\mathbf{k}/\mathrm{d}t = -\partial\omega/\partial\mathbf{x}$. In eikonal theory the phase velocity plays no role, and the overall phase of the wave does not appear in the equations. This is an advantage over modal theories which attempt to obtain position space information, since wave phases are ususally very sensitive to error propagation.

A derivation of the eikonal equations is presented in Section 2, and a further discussion of the equations is given in Section 3. It is convenient to use an interpretation that is slightly different from that which is standard in fluid mechanics. The differences allow the techniques of classical particle mechanics to be used in their textbook form. The eikonal equations follow the evolution of waves which are small in amplitude and have space and/or time scales which are shorter than anything they interact with. The small amplitude allows them to be treated linearly, and the small size allows a perturbation expansion in the scale ratio ε. The eikonal equations match exactly the first two nontrivial powers of ε.

To apply the eikonal to the induced diffusion problem, we imagine the flow to be the sum of a given background and a perturbation. The background is not to be identified with the mean flow, but rather the mean flow is the sum of background plus Stokes drift. The perturbation is a superposition of a set of test wave packets, each with a position (e.g., its center) and a wavenumber (e.g., the mean wavenumber of the packet). Each test wave carries its own amount of action, A. This amount of action is conserved. The energy of the test wave packet is $A\omega$ and its momentum is $A\mathbf{k}$. ω is the total

frequency, including the Doppler shift; $\omega = \sigma + \mathbf{k} \cdot \mathbf{v}_0$ (where σ is the intrinsic frequency, given as a dispersion relation, and $\mathbf{v}_0$ is the background velocity flow). Similarly, two energies can be defined, the "intrinsic energy" $E_i = A\sigma$ (a relation derived by Garrett (1967)), and the "total energy" $E = A\omega$. This latter energy is the more fundamental quantity since E is equal to a Hamiltonian, $H(\mathbf{x}, A\mathbf{k})$, where $\mathbf{x}$ and $A\mathbf{k}$ are canonically conjugate variables. To order ε^2, the only response of the background to the waves is by exchange of mass and momentum (which imply the exchange of energy); we say that the background and the waves are "dynamically independent".

The value of A scales out of the equations of motion, so the amount of action in each packet is arbitrary. As a consequence we can consider $h(\mathbf{x}, \mathbf{k}) = H/A$ as the Hamiltonian and $\mathbf{x}$ and $\mathbf{k}$ as conjugate variables. $\omega = h(\mathbf{x}, \mathbf{k})$ is the dispersion relation for the waves, including Doppler shift. The total energy and momentum are obtained by multiplying ω and $\mathbf{k}$ by A.

The equations of motion for the packet are Hamilton's equations:

$$\frac{\mathrm{d}\mathbf{x}}{\mathrm{d}t} = \frac{\partial h}{\partial \mathbf{k}} \text{ and } \frac{\mathrm{d}\mathbf{k}}{\mathrm{d}t} = -\frac{\partial h}{\partial \mathbf{x}}$$

from which it follows that

$$\frac{\mathrm{d}\omega}{\mathrm{d}t} = \frac{\partial h}{\partial t}$$

In eikonal theory the phase velocity plays no role, and the overall phase of the wave does not appear in the equations. Phase differences are formally given by

$$\Delta\phi = \int_{\substack{\text{initial} \\ \text{point}}}^{\text{final}} \omega \mathrm{d}t + \mathbf{k} \cdot \mathrm{d}\mathbf{x}$$

but inconsequential differences between calculated and true values of ω and $\mathbf{k}$ can make the calculated value of $\Delta\phi$ over any reasonably long path differ significantly from its true value. Moreover, each caustic, of which many must exist in the ocean, causes this expression to be wrong by an extra $\pi/2$ phase shift. The inability to follow the phase is, in fact, a strong point of the eikonal method, since the phase is physically very sensitive to everything. In mode calculations, the phase must be followed very closely in order to reconstruct position information (assuming the position of the test wave is important for its dynamics).

In Section 4 we describe a numerical experiment which consists of following the motion of the center of a wave packet as it propagates through a Garrett–Munk field of internal waves. This section begins with a summary of the essential results of the eikonal derivation and can be read as a self-contained unit. (However, a full appreciation of the underlying ap-

proximations requires an understanding of Sections 2 and 3.) The initial wavenumber and frequency of the wave packet are chosen to lie within the induced diffusion domain. The background flow field is a superposition of 50 linear internal waves chosen by Monte Carlo sampling of the GM-79 model spectrum. Such a flow is predominantly horizontal. Integration of Hamilton's equations, which are six coupled ordinary differential equations, yields the desired motion of the packet. Average properties are obtained by averaging over 50 individual trajectories.

The results of our numerical experiment, as well as other experiments not presented here, show that horizontal transport is unimportant. For example, the wave packet moves with an average horizontal speed of only one-tenth that of a typical Garrett–Munk wave group. On the other hand, changes in vertical wavenumber magnitude, k_v, are very significant. We find a mean motion of k_v to large values, with the same sign as at $t = 0$, and fluctuations about that mean. The individual excursions in k_v are of large magnitude and are a striking feature of the results: an absorbing barrier was placed at $2\pi/k_v = 5$ m, so that if the vertical wavelength of a trajectory falls beneath this cut-off value the trajectory is halted and the initial conditions are reset. Thirty four out of 50 trajectories in our sample surged through the cut-off in a time of less than five inertial periods (our time limit for the integrations). We call such events "critical layer" events because the intrinsic frequency, σ, is close to the inertial frequency, and the wave is almost always behaving in essentially the same way as one that is approaching a critical layer in a time and horizontal position independent shear flow. The existence of a large mean motion of k_v, and the size of the individual excursions, both show that the traditional idea of diffusion in k_v–t space, implying a random walk, is inappropriate. On the basis of our numerical results we provide a simple model which describes much of the transport that occurs. We argue that diffusion actually occurs in σ–z space, and we close by deriving an expression for the probability density of critical layers.

2. DERIVATION OF EIKONAL EQUATIONS

In this section we derive the eikonal equations for a fluid. These follow the evolution of waves which are small in amplitude and have space and/or time scales which are shorter than anything they interact with.

For a systematic development, it is convenient to start with a Hamiltonian description of the fluid flow. A number of Hamiltonian descriptions of continuum fields have been given (Seliger and Whitham, 1968; Miles, 1977; Morrison and Greene, 1980; Henyey, 1981). All such descriptions lead to Hamiltonian densities which can be written in the form

$$\mathscr{H}(\mathbf{q}, \mathbf{p}, \nabla\mathbf{q}, \nabla\mathbf{p}, \boldsymbol{\phi}, \nabla\boldsymbol{\phi}) \tag{1}$$

$\mathbf{q}$ and $\mathbf{p}$ are canonical variables, and $\boldsymbol{\phi}$ (not normally included in the textbook derivations) a subsidiary variable which allows $\mathscr{H}$ to be written in terms of first derivatives. ($\nabla\mathbf{q}$, etc., means any derivative of any component of $\mathbf{q}$). Equations for the flow follow from a variational principle for the action, S:

$$0 = \delta S$$
$$= \delta \int \mathrm{d}t \mathrm{d}^3\mathbf{x}(\mathbf{p} \cdot \partial_t \mathbf{q} - \mathscr{H}) \tag{2}$$

The equations are

$$-\partial_t \mathbf{p} = \frac{\delta H}{\delta \mathbf{q}}$$

$$\partial_t \mathbf{q} = \frac{\delta H}{\delta \mathbf{p}}$$

$$0 = \frac{\delta H}{\delta \boldsymbol{\phi}} \tag{3}$$

where

$$\frac{\delta H}{\delta \mathbf{q}} = \frac{\partial \mathscr{H}}{\partial \mathbf{q}} - \frac{\nabla \cdot \partial \mathscr{H}}{\partial(\nabla \mathbf{q})} \quad \text{etc.} \tag{4}$$

Henyey (1981) has derived the Hamiltonian density for a stratified fluid in the incompressible, Boussinesq, f-plane, and dissipation-free approximations. With the reference density, ρ_0, taken to be unity, the result is

$$\mathscr{H} = \mathbf{v}^2/2 + U(\zeta) \tag{5}$$

The potential energy term, $U(\zeta)$, depends only on the vertical Lagrangian displacement, ζ (one of the canonical coordinates);

$$U(\zeta) = \left(\zeta^2/2 + \zeta^3/6\partial_z\right) N^2(z - \zeta) \tag{6}$$

For deep ocean internal waves, amplitudes are small compared with the scale of variation of the Vaisala frequency (1.3 km), therefore, it is sufficient for our purposes to retain only the quadratic term in U, i.e.,

$$U(\zeta) = \zeta^2/2N^2(z) \tag{7}$$

The velocity, $\mathbf{v}$, is a nonlinear function of $\mathbf{p}$, $\mathbf{q}$, ϕ and their derivatives ($\mathbf{p}$ and $\mathbf{q}$ are two-dimensional vectors for internal waves, and ϕ is a scalar (Henyey, 1981)). Its precise form is not important here. What is important is that all the nonlinearity in $\mathbf{v}$ occurs as the advective combination $-\mathbf{p} \cdot \nabla\mathbf{q}$:

$$\mathbf{v}(\mathbf{p}, \mathbf{q}, \phi) = \mathbf{v}_l - \mathbf{p} \cdot \nabla\mathbf{q} \tag{8}$$

where $\mathbf{v}_l$ is a linear combination of $\mathbf{p}$, $\mathbf{q}$, and ϕ.

Our specific interest is an eikonal description of "induced diffusion". The physical description of this process involves a restricted set of interactions,

between small-scale, high-frequency "test waves" and a much larger scale low-frequency background flow (McComas and Bretherton, 1977). The test waves are to be considered as small amplitude perturbations on the background flow. Because of the small amplitudes, interaction between the test waves is unimportant. Therefore, it suffices to follow the test waves to first order in their amplitude, a. For this purpose the Hamiltonian is truncated at quadratic order, $\mathcal{O}(a^2)$, retaining all orders in the background. To $\mathcal{O}(a)$ the influence of the test waves on the background is dropped. We assume the $\mathcal{O}(a)$ background flow to be a specified solution of the equations of motion without the perturbation. At this stage, it is important to imagine the background to be an exact solution at orders below $\mathcal{O}(a^2)$; at a later stage we can replace it with an approximate solution. Later, we will discuss the $\mathcal{O}(a^2)$ influence of the test wave on the background.

We perform, therefore, a canonical transformation

$$\mathbf{p} \to \mathbf{p}_0 + \mathbf{p}$$
$$\mathbf{q} \to \mathbf{q}_0 + \mathbf{q}$$
$$\phi \to \phi_0 + \phi \tag{9}$$

on the action

$$S = \int \mathrm{d}t \mathrm{d}^3\mathbf{x}(\mathbf{p} \cdot \dot{\mathbf{q}} - \mathscr{H}) \tag{10}$$

Quantities with subscript 0 refer to the given background flow, and quantities without subscripts refer to the test wave perturbation. The latter quantities are the dynamical variables and we wish to retain these only up to quadratic terms.

Terms independent of the dynamical variables give a contribution to S that has no variation when the values of $\mathbf{p}$, $\mathbf{q}$, and ϕ are varied. Such contributions can, therefore, be dropped. Linear terms in the perturbation do not contribute to S (except at the boundaries at which a variation is not performed), since the background is an exact solution of $\delta S = 0$. Thus, only the quadratic terms are left.

In the quadratic terms, we make one further approximation, consistent with the eikonal approximation made below. When the expansion (9) is substituted into terms of the form $\mathbf{v} \cdot \mathbf{p}\nabla\mathbf{q}$ in the kinetic energy, either $\mathbf{v}$, $\mathbf{p}$, or $\mathbf{q}$, can have subscript zero. The test wave variables are assumed to have much larger wavenumbers than the background. Thus, the term with $\mathbf{q}_0$ can be dropped relative to terms with $\mathbf{q}$. Upon integration by parts, $\mathbf{v} \cdot \mathbf{p}\nabla\mathbf{q} \to -\mathbf{v} \cdot \mathbf{q}\nabla\mathbf{p}$ (since $\nabla \cdot \mathbf{v} = 0$). It follows, therefore, that the terms in $\mathbf{p}_0$ can also be dropped, and the induced diffusion approximation has led us to replace $\mathbf{v} \cdot \mathbf{p}\nabla\mathbf{q}$ by $\mathbf{v}_0 \cdot \mathbf{p}\nabla\mathbf{q}$.

With the set of approximations made, the action has the form

$$S = \int \mathrm{d}t \mathrm{d}^3\mathbf{x}\, \mathbf{p} \cdot (\partial_t + \mathbf{v}_0 \cdot \nabla)\mathbf{q} - \mathscr{h}(\mathbf{p}, \mathbf{q}, \phi) \tag{11}$$

where $\mathcal{H}$ is the quadratic Hamiltonian density in the absence of the background. The only interaction is in the replacement of the partial time derivative by the substantive derivative.

$$d_t = \partial_t + \mathbf{v}_0 \cdot \nabla \tag{12}$$

If the nonlinear terms in the potential energy or the remaining terms from the expansion of $\mathbf{v} \cdot \mathbf{p}\nabla\mathbf{q}$ had been retained, there would be additional coupling of the test wave to the background. The coupling retained in (12) is essentially the same as in the Taylor–Goldstein equation. (Slight differences are due to the lack of commutation of the operators d_t and ∇. The contributions of their commutator are of the same order as neglected terms.)

Now that we have eq. 11, we can replace the exact $\mathbf{v}_0$ by an approximate solution, such as neglect of the vertical component of $\mathbf{v}_0$. If this approximation had been made earlier, the test wave dynamics would be incorrect due to the attempt of the test wave equation to compensate for the approximate background.

We now have a Hamiltonian which is quadratic in the dynamical variables, with coefficients that may be space and time dependent (via the specified background flow). In case the reader dislikes one or more of the approximations we have made so far, we will develop the eikonal approximation for a general quadratic Hamiltonian. This demonstrates that the essentials of the eikonal theory are independent of these approximations.

To simplify notation, we combine $\mathbf{p}$, $\mathbf{q}$ and $\boldsymbol{\phi}$ into a new vector, $\mathbf{z}$

$$\mathbf{z} = (\mathbf{p}, \mathbf{q}, \boldsymbol{\phi}) \tag{13}$$

If $\mathbf{p}$ and $\mathbf{q}$ have n elements, and $\boldsymbol{\phi}$ has m elements, then $\mathbf{z}$ has $2n + m$ elements. Hamilton's equation, (3), can be rewritten as

$$\sum_\beta \mathrm{J}_{\alpha\beta}\partial_t z_\beta = \frac{\delta H}{\delta z_\alpha}$$

$$= \frac{\partial \mathscr{H}}{\partial z_\alpha} - \nabla \cdot \frac{\partial \mathscr{H}}{\partial \nabla z_\alpha} \tag{14}$$

where

$$\mathrm{J} = \begin{pmatrix} 0 & \mathrm{I} & 0 \\ -\mathrm{I} & 0 & 0 \\ 0 & 0 & 0 \end{pmatrix} \tag{15}$$

and I is the $n \times n$ identity matrix. The zeros are $n \times n$, $n \times m$, $m \times n$, or $m \times m$ zero matrices. An important property of J is its antisymmetry:

$$\mathrm{J}_{\alpha\beta} = -\mathrm{J}_{\beta\alpha} \tag{16}$$

The most general quadratic Hamiltonian density with no higher than first

derivatives is

$$\mathscr{H} = \tfrac{1}{2} \sum_{\alpha,\beta} \left[A_{\alpha\beta} z_\alpha z_\beta + \mathbf{B}_{\alpha\beta} z_\alpha \cdot \nabla z_\beta + \nabla z_\alpha \cdot \overline{\overline{\mathbf{C}}}_{\alpha\beta} \cdot \nabla z_\beta \right] \tag{17}$$

The scalars, $A_{\alpha\beta}$, vectors, $\mathbf{B}_{\alpha\beta}$, and dyadics, $\overline{\overline{\mathbf{C}}}_{\alpha\beta}$, can explicitly depend on space and time. In our induced diffusion problem, this dependence occurs primarily through the dependence of $\mathbf{B}_{\alpha\beta}$ on the background velocity. There is a slower dependence on depth through the Brunt–Vaisala frequency. In the formal development, we will not restrict the space–time dependence of A, B, or C.

There is no loss of generality in assuming

$$\begin{aligned} A_{\alpha\beta} &= A_{\beta\alpha} \\ \mathbf{B}_{\alpha\beta} &= -\mathbf{B}_{\beta\alpha} \\ \overline{\overline{\mathbf{C}}}_{\alpha\beta} &= \overline{\overline{\mathbf{C}}}_{\beta\alpha}^{\mathrm{T}} \end{aligned} \tag{18}$$

(The superscript T means transpose in the space indices. The α, β indices are shown explicitly transposed). The equations of motion are

$$\sum_\beta \mathbf{J}_{\alpha\beta} \partial_t z_\beta = \sum_\beta \left[A_{\alpha\beta} z_\beta + \tfrac{1}{2} \mathbf{B}_{\alpha\beta} \cdot \nabla z_\beta + \tfrac{1}{2} \nabla \cdot \left(\mathbf{B}_{\alpha\beta} z_\beta \right) - \nabla \cdot \left(\overline{\overline{\mathbf{C}}}_{\alpha\beta} \cdot \nabla z_\beta \right) \right] \tag{19}$$

This is a linear equation, so solutions superpose. We decompose the field of waves into a superposition of overlapping wave packets, more or less filling the available space. Each packet is somewhat localized in space, but is large enough to contain several wavelengths. Each packet has a narrow band of wavenumbers, centered on the nominal wavenumber, $\mathbf{k}$, of the packet. The eikonal approximation is applied to each packet separately.

The eikonal technique involves the ansatz

$$z_\alpha = \mathscr{R}\mathrm{e}\left(a_\alpha \mathrm{e}^{iS} \right) \tag{20}$$

and a scale separation which asserts that the factor e^{iS} varies much more rapidly than either a_α or the coefficients A, B and C. This scale separation can be expressed as a formal asymptotic expansion by associating a scale separation factor, ε, with each derivative in eq. 19 and replacing S in eq. 20 by S/ε, and expanding in powers of ε. It is convenient to put all the ε dependence into a_α (on occasion other choices have been made in the literature):

$$a_\alpha = a_\alpha^{(0)} + \varepsilon a_\alpha^{(1)} + \ldots \tag{21}$$

Since eq. 19 is linear, we can ensure that $a_\alpha^{(1)}$ is orthogonal to $a_\alpha^{(0)}$. Thus

$$\sum_\alpha a_\alpha^{(0)*} a_\alpha^{(1)} = 0 \tag{22}$$

where * means complex conjugate.

We assume that $a_\alpha e^{iS}$ (real *and* imaginary parts) obeys (19). The $\mathcal{O}(1)$ terms of (19), divided by e^{iS}, give

$$\sum_\beta M_{\alpha\beta} a_\beta^{(0)} = 0 \tag{23}$$

where

$$M_{\alpha\beta} = -i\omega J_{\alpha\beta} - A_{\alpha\beta} - i\mathbf{B}_{\alpha\beta}\cdot\mathbf{k} - \mathbf{k}\cdot\overline{\overline{\mathbf{C}}}_{\alpha\beta}\cdot\mathbf{k} \tag{24}$$

and

$$\omega = -\frac{\partial S}{\partial t} \tag{25}$$

$$\mathbf{k} = \nabla S \tag{26}$$

The lowest order solution, $a_\alpha^{(0)}$, is determined as an eigenvector with vanishing eigenvalue of a Hermitian matrix, $M_{\alpha\beta}$. (The Hermiticity is a consequence of eqs. 16 and 18.) The condition for existence of the eigenvalue is

$$\det M = 0 \tag{27}$$

which is an equation that relates ω and $\mathbf{k}$. The roots of this equation are the dispersion relations for the various types of disturbance possible. We will select the root for internal waves rather than the root for horizontal eddy motion.

The $\mathcal{O}(\varepsilon)$ part of (19), divided by e^{iS}, is

$$\sum_\beta \Big[M_{\alpha\beta} a_\beta^{(1)} + J_{\alpha\beta}\partial_t a_\beta^{(0)} - \tfrac{1}{2}\big(\nabla\cdot\mathbf{B}_{\alpha\beta}\big) a_\beta^{(0)} - \mathbf{B}_{\alpha\beta}\cdot\nabla a_\beta^{(0)} + \nabla\cdot\big(\overline{\overline{\mathbf{C}}}_{\alpha\beta}\cdot i\mathbf{k}\big) a_\beta^{(0)} + 2\big(\overline{\overline{\mathbf{C}}}_{\alpha\beta}\cdot i\mathbf{k}\big)\cdot\nabla a_\beta^{(0)} \Big] = 0 \tag{28}$$

The components of this equation orthogonal to $a_\alpha^{(0)}$ serve to set the values for $a_\alpha^{(1)}$, but do not constrain $a_\alpha^{(0)}$. The component along $a_\alpha^{(0)}$, however, is independent of $a_\alpha^{(1)}$, and is a condition on $a_\alpha^{(0)}$. Multiplying (28) by $-i/2a_\alpha^{(0)*}$ and summing on α gives (on taking the real part; the imaginary part vanishes):

$$\partial_t\left[-\frac{i}{4}\sum_{\alpha,\beta} a_\alpha^{(0)*} J_{\alpha\beta} a_\beta^{(0)}\right] + \nabla\cdot\frac{i}{4}\sum_{\alpha,\beta} a_\alpha^{(0)*}\Big[\mathbf{B}_{\alpha\beta} - 2i\mathbf{k}\cdot\overline{\overline{\mathbf{C}}}_{\alpha\beta}\Big] a_\beta^{(0)} = 0 \tag{29}$$

This has the form of a conservation equation

$$\partial_t \mathscr{A} + \nabla\cdot(\mathbf{v}\mathscr{A}) = 0 \tag{30}$$

$\mathscr{A}$ is the action density

$$\mathscr{A} = \frac{-i}{4}\sum_{\alpha,\beta} a_\alpha^{(0)*} J_{\alpha\beta} a_\beta^{(0)}$$

$$= \frac{-i}{4}(\mathbf{p}^* \cdot \mathbf{q} - \mathbf{q}^* \cdot \mathbf{p}) \tag{31}$$

and $\mathbf{v}$ is the velocity of action flow. The velocity of action flow can be identified with the group velocity of the waves as follows: differentiate (23) with respect to the wavenumber, $\mathbf{k}$, multiply by $1/4\ a_\alpha^{(0)*}$, sum on α, and use the conjugate of (23) to eliminate the term

$$\tfrac{1}{4} \sum_{\alpha,\beta} a_\alpha^{(0)*} \mathrm{M}_{\alpha\beta} \frac{\partial a_\beta^{(0)}}{\partial \mathbf{k}}$$

We obtain

$$0 = \sum_{\alpha,\beta} \tfrac{1}{4} a_\alpha^{(0)*} \frac{\partial \mathrm{M}_{\alpha\beta}}{\partial \mathbf{k}} a_\beta^{(0)}$$

$$= \sum_{\alpha,\beta} \left[-\frac{i}{4} \frac{\partial \omega}{\partial \mathbf{k}} a_\alpha^{(0)} \mathrm{J}_{\alpha\beta} a_\beta^{(0)} - \tfrac{1}{4} a_\alpha^{(0)*} \left(-i\mathbf{B}_{\alpha\beta} - 2\overline{\overline{\mathbf{C}}}_{\alpha\beta} \cdot \mathbf{k} \right) a_\beta^{(0)} \right.$$

$$\left. = \mathscr{A} \frac{\partial \omega}{\partial \mathbf{k}} - \mathscr{A} \mathbf{v} \right] \tag{32}$$

Thus, we have the important relation

$$\mathbf{v} = \frac{\partial \omega}{\partial \mathbf{k}} \tag{33}$$

The phase, S, is eliminated from the basic set of equations (in favor of ω and $\mathbf{k}$) by replacing eqs. 25 and 26 by their conditions of integrability

$$\frac{\partial \mathbf{k}}{\partial t} = -\nabla \omega \tag{34}$$

$$\nabla \times \mathbf{k} = 0 \tag{35}$$

Each wavepacket moves with velocity, $\mathbf{v}$. In order to follow a wavepacket, we should know how its wavenumber changes, which is

$$\frac{\mathrm{d}\mathbf{k}}{\mathrm{d}t} = \frac{\partial \mathbf{k}}{\partial t} + \mathbf{v} \cdot \nabla \mathbf{k} \tag{36}$$

Using eqs. 33 and 34, we obtain

$$\frac{\mathrm{d}\mathbf{k}}{\mathrm{d}t} = -\nabla \omega + \frac{\partial \omega}{\partial \mathbf{k}} \cdot \nabla \mathbf{k} \tag{37}$$

The dispersion relation gives ω as a function of $\mathbf{k}$, $\mathbf{x}$ and t. Hence

$$\nabla \omega = \frac{\partial \omega}{\partial \mathbf{x}} + \nabla \mathbf{k} \cdot \frac{\partial \omega}{\partial \mathbf{k}} \tag{38}$$

Therefore, using (35) ($\nabla \mathbf{k}$ is a symmetric dyadic),

$$\frac{d\mathbf{k}}{dt} = -\frac{\partial \omega}{\partial \mathbf{x}} \tag{39}$$

and (33) can be rewritten as

$$\frac{d\mathbf{x}}{dt} = \frac{\partial \omega}{\partial \mathbf{k}} \tag{40}$$

Equations 39 and 40 are Hamilton's equations, with ω a Hamiltonian given by the dispersion relation. $\mathbf{x}$ and $\mathbf{k}$ are the canonically conjugate variables. These equations are the fundamental equations we integrate to find the motion of the wave packet in $\mathbf{x}$, $\mathbf{k}$ space. For interpretational purposes, these equations should be modified so that the Hamiltonian is the energy of the wave packet. The energy density is obtained by replacing z in eq. 17 by $(ae^{iS} + a^* e^{-iS})/2$. To leading order, the derivatives act only on the $e^{\pm iS}$. The energy density contains slowly varying parts coming from cross terms between ae^{iS} and $a^* e^{-iS}$, as well as rapidly fluctuating terms proportional to $e^{\pm 2iS}$. The rapidly fluctuating terms integrate to zero (up to corrections which vanish exponentially with the expansion parameter), so the total energy can be computed from the slowly varying parts. Upon integration by parts, we can write the energy density to leading order as

$$\mathscr{E} = \tfrac{1}{4} \sum_{\alpha,\beta} a_\alpha^{(0)*} \left[A_{\alpha\beta} + i\mathbf{k} \cdot \mathbf{B}_{\alpha\beta} + \mathbf{k} \cdot \overline{\overline{\mathbf{C}}}_{\alpha\beta} \cdot \mathbf{k} \right] a_\beta^{(0)} \tag{41}$$

From (23), (24), and (31), this can be rewritten as

$$\mathscr{E} = \mathscr{A}\omega \tag{42}$$

Integrating over the wavepacket gives

$$E = A\omega \tag{43}$$

where

$$E \equiv \int d^3\mathbf{x}\, \mathscr{E};\ A \equiv \int d^3\mathbf{x}\, \mathscr{A} \tag{44}$$

and where $\omega \equiv \langle \omega \rangle = 1/A \int d^3\mathbf{x}\, \omega \mathscr{A}$ is the weighted average of ω at each point. We are imagining the situation when the values of ω are essentially constant over the packet. A is the conserved action of the wave packet, $dA/dt = 0$, and E is the energy. Equation 43 is almost, but not quite, Garrett's relation between energy and action (see next section). We have derived (43) and action conservation in a general context; one need not verify them separately for each system, as has been the practice in the literature. The condition for the validity of (43) in the eikonal approximation is merely that the system has a Hamiltonian. This is known to be true for a wide class of continuum systems, as long as dissipation processes are neglected.

If we write

$$H = A\omega(\mathbf{k}, \mathbf{x}, t) \tag{45}$$

and

$$\mathbf{p} = A\mathbf{k} \tag{46}$$

then Hamilton's equation, (39) and (40) can be expressed in terms of the Hamiltonian which is the energy of the wave packet as

$$\frac{\mathrm{d}\mathbf{p}}{\mathrm{d}t} = -\frac{\partial H}{\partial \mathbf{x}} \tag{47}$$

$$\frac{\mathrm{d}\mathbf{x}}{\mathrm{d}t} = \frac{\partial H}{\partial \mathbf{p}} \tag{48}$$

From these equations, one sees that $\mathbf{p}$ is the momentum of the wave packet.

The quantity $\mathbf{p}$ has been called a "pseudo-momentum", and its interpretation as a true momentum has even been labeled a "myth" (McIntyre, 1981). Since we accept this myth as true, some discussion is appropriate. It turns out that this point is closely related to the connection between our expression, $E = A\omega$, and Garrett's expression, and to the interaction being entirely in the replacement $\partial_t \to \partial_t + \mathbf{v}_0 \cdot \nabla$, and to the Stokes drift. These topics form the subject matter of the next section.

A complete set of equations in the eikonal approximation is comprised of Hamilton's equations, action conservation, and $\nabla \times \mathbf{k} = 0$. This last equation is the condition that a family of trajectories describing the detailed motion of one packet forms a normal family. This condition is important for image-forming optical systems (Landau and Lifshitz, 1975), but is of no particular significance in the transport theory of a random collection of waves. The equation, $\nabla \times \mathbf{k} = 0$, is consistent with Hamilton's equations; if it is imposed at the initial time, it holds true at later times. We will consider wave packets sufficiently small that at $t = 0$ we can assume $\mathbf{k}$ to be constant, so, $\nabla \times \mathbf{k}$ is trivially zero intially. Furthermore, we only follow the central position of the wave packets, and, since we are not following phases, we can consider dispersion as an exchange of action between different packets.

3. THE STOKES DRIFT, TOTAL ENERGY AND INTRINSIC ENERGY

In the previous Section, the following results were obtained:

(1) if the continuum system is describable by a Hamiltonian, then the eikonal approximation can be made (Whether or not it is accurate is another matter.);

(2) there is a conserved action, A, which flows with a group velocity;

(3) the energy is $A\omega$ and the momentum is $A\mathbf{k}$;

(4) the frequency expressed as a function of $\mathbf{k}$ and $\mathbf{x}$ is a Hamiltonian. By rescaling with the action, the Hamiltonian is the energy; and

(5) under a reasonable set of approximations, the interaction with the background flow, $\mathbf{v}_0$, is obtained by replacing ∂_t by $\partial_t + \mathbf{v}_0 \cdot \nabla$.

The results 1 to 4 have been obtained in a more general framework than result 5. For the purposes of the remainder of this paper, we accept result 5, which applies not only to our problem, but with similar approximations to many wave systems in which the waves are disturbances of a material medium. Essentially, all of the fluid dynamics literature on action conservation, etc., has been concerned with such systems.

The eikonal approximation that follows from result 5 involves a dispersion relation

$$\omega = \sigma(\mathbf{k}) + \mathbf{v}_0 \cdot \mathbf{k} \tag{49}$$

where $\sigma(\mathbf{k})$ is the dispersion relation in the absence of the background flow, $\mathbf{v}_0$. The extra term is the Doppler shift induced by the flow. Following conventional terminology we call σ the intrinsic frequency and ω the total frequency. Multiplying each of these by the action of a wavepacket we obtain an energy associated with the wavepacket. By analogy with the terminology for frequencies, we call these the intrinsic and total energies of the packet. Garrett's relation (Garrett, 1967) is

$$E_i = A\sigma \tag{50}$$

whereas the relation derived in the previous section is $E = A\omega$. The difference between E and E_i is given in terms of eq. 49 and the expression (46) for the momentum as

$$E = E_i + \mathbf{v}_0 \cdot \mathbf{p} \tag{51}$$

Hence, the nature of E is related to the nature of $\mathbf{p}$.

The momentum, $\mathbf{p}$, has been introduced as the canonical momentum—the quantity conjugate to the position $\mathbf{x}$, or equivalently as the generator of infinitesimal displacements of position. If one makes a microscopic theory of a fluid, the momentum, defined in the same way, is the mass times the velocity:

$$\mathbf{p} = \int d^3\mathbf{x}\,\rho\mathbf{v} \tag{52}$$

(The total velocity is $\mathbf{v}_0 + \mathbf{v}$). We will show the equivalence of expressions (46) and (52) (through quadratic order, which is the order at which action is usually defined), thereby demonstrating that $\mathbf{p}$ is a true momentum, not a pseudomomentum. In fact, $\mathbf{p}$ turns out to be the Stokes drift of the wavefield.

The existence of the Stokes drift has been questioned for wavefields other than surface waves. This issue is clarified by noticing that the decomposition

into background and wavefield is not the same as the decomposition into mean flow and fluctuating flow, since the fluid velocity is nonlinear in the canonical variables. (The quadratic part of $\mathbf{v}$ has to be retained when evaluating (52) because of the constant term in ρ.) The decomposition (to $\mathcal{O}(a^2)$) into background and wavefield proceeds as follows. The canonical variables (rather than velocity components) are Fourier transformed into wavenumber space (Fourier transforming is a canonical transformation), then projected into small wavenumber components (background) and large wavenumber components (wave field). The two sets of components are then Fourier transformed separately, back into position space. As a result, the *canonical* variables of the wave field are decomposed into mean and fluctuating parts. By construction, Poisson brackets between background and wave field vanish; the different scales are dynamically independent.

The mean momentum (or mean velocity in the incompressible, Boussinesq approximations) can be evaluated. The mean momentum of the background is obtained from terms in the momentum that are independent of the wave field. Terms linear in the wave field canonical variables are fluctuating quantities, and average to zero. There is a contribution to the average momentum from the wave field. This is the Stokes drift, i.e., the mass flow associated with the wave field. It comes from the quadratic terms in $\rho\,\mathbf{v}$:

$$\langle (\rho \mathbf{v})_{\text{quad}} \rangle = \langle p \nabla q \rangle \tag{53}$$

$$= \left\langle \left(\frac{a_p + a_p^*}{2} \right) \left(\frac{i\mathbf{k} a_q - i\mathbf{k} a_q^*}{2} \right) \right\rangle \tag{54}$$

$$= \frac{\mathbf{i}\mathbf{k}}{4} \left(a_p^* a_q - a_q^* a_p \right) \tag{55}$$

$$= \mathbf{k} A \tag{56}$$

where $\langle \ldots \rangle$ denotes the projection described above. Thus, the microscopic definition of the momentum of the wave field agrees with the definition as generator of space translation.

A physical interpretation of this result is that the Stokes drift accompanies the waves, while the background is dynamically independent. Thus, for example, if initial conditions consist of a fluctuating wave packet and zero mean flow, the Stokes drift ($A\mathbf{k}$) will move with the packet, while the background ($-A\mathbf{k}$ at $t = 0$) will evolve separately. The (negative of the) divergence of the Stokes drift is a source of flow for the background, $-\mathrm{d}/\mathrm{d}t$ ($A\mathbf{k}$) is a force on the background, and $-\mathrm{d}/\mathrm{d}t$ ($A\omega$) is work done on the background. Thus the background flow responds indirectly to the wave field. The relationship of the background flow to the Stokes drift depends on the geometry of the wave field envelope. An extreme case is a wave packet much longer in the $\mathbf{k}$ direction than in the other two directions. In this instance,

illustrated in Fig. 1, the Stokes drift deposits water at one end of the packet and depletes it from the other end. The background includes a dipole return flow between this source and sink. The return flow occupies a region much larger than the wave packet, and is much weaker. The total flux of the return flow cancels the total flux of the Stokes drift, as required by the equation of continuity. A second extreme case, also illustrated in Fig. 1, is a wave packet much shorter in the **k** direction than in the other two directions. In this case, the source and sink are spread out over the two sides of the flattened packet, and the return flow cancels the Stokes drift, leaving nearly zero mean flow.

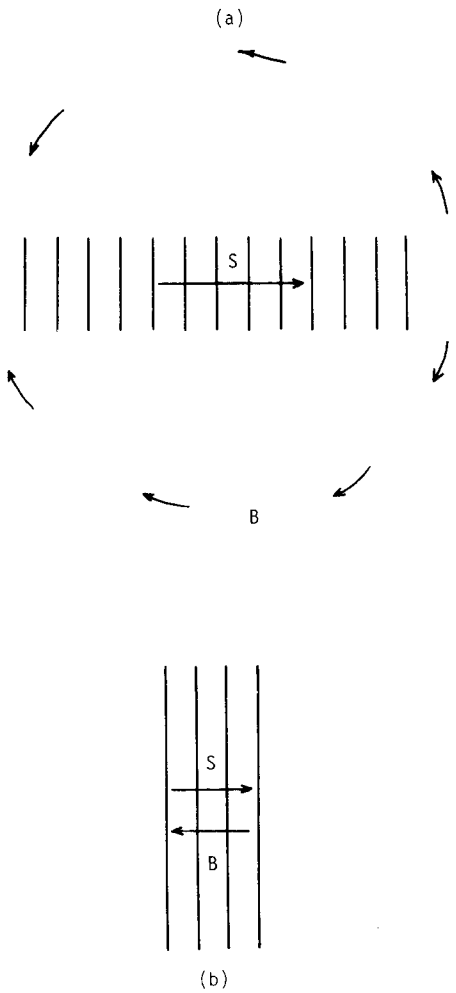

Fig. 1. The Stokes drift (S) and background (B) in two extreme cases. In case (a), when the wave packet is elongated in the wavenumber direction, the Stokes drift is much larger and more concentrated than the background. In case (b), when the wave packet is flattened in the **k** direction, the background nearly cancels the Stokes drift, and the mean flow is nearly zero.

We are now in a position to understand the difference between the intrinsic and total energies of the wave field. The intrinsic energy is the potential energy of the wave field plus the kinetic energy of the fluctuating part. This is the traditional energy, and is appropriate in the mean/fluctuating decomposition. In the background/wave decomposition, however, the Stokes drift is associated with the wave. The total energy of the wave is, by definition, the difference of the total energy and the energy of the background. The wave kinetic energy contains, in addition to the part in E_i, the contribution

$$\int d^3\mathbf{x}\left(\tfrac{1}{2}\rho v^2_{\text{mean}} - \tfrac{1}{2}\rho v^2_{\text{background}}\right)$$

$$= \int d^3\mathbf{x}\tfrac{1}{2}\rho\left[(\mathbf{v}_0 + \mathbf{v}_{\text{Stokes}})^2 - v_0^2\right] \tag{57}$$

$$= \int d^3\mathbf{x}(\mathbf{v}_0 \cdot \mathbf{v}_{\text{Stokes}}) \tag{58}$$

to the order we are calculating. Therefore

$$E - E_i = \int d^3\mathbf{x}\rho(\mathbf{v}_0 \cdot \mathbf{v}_{\text{Stokes}}) \tag{59}$$

$$= \mathbf{v}_0 \cdot \mathbf{p} \tag{60}$$

which is identical to (51).

The choice between canonical decomposition, using $\mathbf{k}$, ω, $\mathbf{p}$ and E, or mean/fluctuating decomposition, using $\mathbf{k}$, σ, no momentum and E_i, may seem arbitrary. Indeed, either can be used correctly. However, there are a number of simplifying features of the canonical decomposition not shared by the other decomposition. These are:

(1) $E = H$. The energy is the value of the Hamiltonian;

(2) the flux of action, momentum, or energy is the group velocity times the density of the same quantity;

(3) as a consequence, the sources of momentum and energy of the background from the waves are $-d_t\mathbf{p}$ and $-d_t E$, respectively. The source of mass is $-\nabla \cdot \mathbf{p}$, the divergence of the Stokes drift;

$$(4)\ d_t\mathbf{p} = -\partial_x H;\ d_t E = \partial_t H. \tag{61}$$

According to classical mechanics, the only changes in momentum and energy come from explicit dependence on space and time. Thus, for example, E (but not E_i) is conserved in motion through a steady, but position-dependent, background flow. In the case of $\partial_x\sigma = 0$ (by assuming constant Brunt–Vaisala frequency), these equations are

$$d_t\mathbf{p} = -\nabla\mathbf{v}_0 \cdot \mathbf{p};\ d_t E = \partial_t\mathbf{v}_0 \cdot \mathbf{p} \tag{62}$$

(5) the approximation scheme does not destroy action conservation; and

(6) the general relations $E = A\omega$ and $\mathbf{p} = A\mathbf{k}$ hold even if the approxima-

tions which gave $\omega = \sigma + \mathbf{k} \cdot \mathbf{v}_0$ are not made. The canonical formulation of the eikonal is more general than is the mean/fluctuating formulation.

4. THE OCEAN MODEL, COMPUTATION PROCEDURES, RESULTS, AND DISCUSSION

We wish to study the motion of the center of a wave packet as it propagates through a field of internal waves. This motion is given as the solution of Hamilton's equations, $d\mathbf{k}/dt = -\partial\omega/\partial\mathbf{x}$ and $d\mathbf{x}/dt = \partial\omega/\partial\mathbf{k}$, which were derived in Section 2 as eqs. 39 and 40. The Hamiltonian which governs the motion is $\omega = \sigma(\mathbf{k}) + \mathbf{v}_0 \cdot \mathbf{k}$, as explained in Section 3. A factor, A, of wave action, constant along the trajectory, has been scaled out.

The dispersion relation for linear internal waves is

$$\sigma(\mathbf{k}) = \left(\frac{k_h^2 N^2 + k_v^2 f^2}{k_h^2 + k_v^2} \right)^{1/2} \tag{63}$$

where $\mathbf{k}_h$ and k_v are the horizontal and vertical components of wavenumber $\mathbf{k}$. For the induced diffusion model the flow field consists of large and small scale components. Using the notation of Meiss and Watson, we let $\mathbf{k}$ represent a wavenumber of the small-scale (test wave) flow, and $\mathbf{l}$ represent a wavenumber of the large-scale (background) flow. The induced diffusion interactions are characterized by the inequalities

$$k_h \gg l_h, k_v \gg l_v, \sigma(k) \gg \sigma(l) \tag{64}$$

It is a good approximation to neglect the vertical velocity of the background.

An initial condition ($\mathbf{k}$, $\mathbf{x}$, $\sigma(k)$) of interest is chosen for the wave packet. The packet propagates through, and interacts with, the background flow, $\mathbf{u}(\mathbf{x}, t)$. However, to the order of interest, the evolution of the background is independent of the packet. To describe the background, we use the best-available model of deep ocean internal wave data (Munk, 1981), namely the Garrett–Munk spectrum. (We use the GM-79 version.) In synthesizing this spectrum, Garrett and Munk assumed an exponential Vaisala profile

$$N(z) = N_0 \exp(z/B) \tag{65}$$

linear wave dynamics, and a WKB approximation for the discrete vertical displacement eigenfunctions. Dimensioned quantities have the values $N_0 = 5.2 \times 10^{-3}$ rad s^{-1}, and $B = 1.3$ km. The vertical component of the Coriolis frequency is $f = 7.3 \times 10^{-5}$ rad s$^{-1} = 0.014 N_0$, corresponding to the latitude of 30°. The horizontal components of the frequency are neglected. The Garrett–Munk spectrum is to be understood as a phenomenological summary of the observed data, only very roughly incorporating dynamics, rather than as a dynamical model of internal waves. We do not expect its deficiencies to

have any important bearing on our considerations of the deep ocean.

Consistent with the observations that went into the making of GM-79, our background flow at the position of the packet is

$$\mathbf{u} = \sum_{j=1}^{NW} \mathbf{u}^{(j)}(\mathbf{x}, t) \tag{66}$$

Each wave component, $\mathbf{u}^{(j)}$, has the form

$$\frac{\mathbf{u}^{(j)}}{N_0 B} = a^{(j)} \left(\hat{l}_h^{(j)} + i \frac{f}{\sigma(l^{(j)})} \hat{l}_h^{(j)} \times \hat{z} \right) \frac{W'(z)^{(j)}}{W'(0)^{(j)}} \exp\left[i \left(\mathbf{l}_h^{(j)} \cdot \mathbf{x}_h - \sigma(l^{(j)}) t \right) \right] \tag{67}$$

Here, W' denotes the z-derivative of the vertical displacement eigenfunction. For a Vaisala profile of the form (65), the WKB expression for this eigenfunction is

$$W(z) \propto \mathrm{e}^{-z/2B} \sin(l_z B + \pi/4) \tag{68}$$

where

$$l_z B = \pi(m - 1/4)\mathrm{e}^{z/B} \tag{69}$$

relates vertical wavenumber, l_z, to equivalent modenumber, m. In eq. 67 the amplitudes $a^{(j)}$ are complex Gaussian random variables with zero mean, and variance $\langle |a^{(j)}|^2 \rangle$ equal to the value which gives

$$\langle u^2 \rangle = 44.0 \frac{N(z)}{N_0} \mathrm{cm}^2\ \mathrm{s}^{-2} \tag{70}$$

corresponding to an r.m.s. current in the upper ocean beneath the mixed layer of 7 cm s^{-1}. Wavenumbers and frequencies of the linear waves which make up the background were chosen by Monte Carlo sampling from the GM-79 spectrum of horizontal velocity. This spectrum is defined by the equations

$$\langle u^2 \rangle = \int \mathrm{d}\sigma \sum_m F_u(\sigma, m) \tag{71}$$

where

$$\frac{F_u}{B^2 N_0^2} = 1.2 \times 10^{-6} N(z) \left(\frac{\sigma^2 + f^2}{\sigma^2} \right) \left(\frac{1}{\sigma(\sigma^2 - f^2)^{1/2}} \right) \left(\frac{1}{m^2 + 9} \right) \tag{72}$$

The probability of choosing a particular vertical modenumber and frequency of a sampled wave incorporates the last two terms in parentheses in eq. 72, while the mean intensity of the Gaussian amplitudes incorporates the first term in parentheses. Thus, most of the background waves that make up **u** have low frequencies and small modenumbers. A modenumber cut-off at

$m = 250$ was imposed as approximately describing the observed 10-m break in the spectrum (Gregg, 1977). The direction of the unit vector, $\hat{\mathbf{l}}_h$, was chosen by sampling from a uniform distribution of angles in $0 \rightarrow 2\pi$. Finally, the number of waves which make up the horizontal background flow was chosen to be $NW = 50$. This choice was based on the requirement that the flow should be relatively smooth and realistic, but also that computation costs should be tolerable; the evaluation of the $NW \times 2$ trigonometric functions, in eq. 66 at each time step of the integration is a major factor in the computing time.

Once the background flow has been constructed and initial values of $\mathbf{k}$, $\mathbf{x}$ and σ for the wave packet are chosen, the six coupled ordinary differential equations (Hamilton's equations) which govern the motion of the packet are numerically integrated using the best-available general purpose algorithm (Shampine and Gordon, 1975). The integration of a given trajectory is halted after a maximum of five inertial periods; $\mathbf{k}$, $\mathbf{x}$ and σ are reset to their initial values, a new realization of the background flow is constructed, and another trajectory is integrated. If the vertical wavelength $\lambda_v = 2\pi/k_v$ becomes "too small" however, (< 5 m) we halt the trajectory and declare it to have "reached a critical layer". We suspect that dissipation processes might set in near this scale, although the dynamics of the induced-diffusion portion of the spectrum we are following is considerably different from the dynamics of the dominant, lower horizontal wavenumber part that is responsible for the 10-m break. With these procedures, a total of 50 trajectories are obtained from which average properties are calculated. All averages are taken over the number of surviving trajectories. The total c.p.u. time for the computation was 16 000 s on a PRIME 500 computer.

Figures 2–7 show results for wave packet initial condition $\mathbf{k}B = (39.89, 0.00, -57.50)$, $\mathbf{x}/B = (0.00, 0.00, -1.00)$, and $\sigma/N_0 = 0.21$; that is, WKB modenumber $m = 50$, initial depth $(-z) = 1.3$ km, and intrinsic frequency $\sigma = 15\, f$.

Figures 2 and 3 show plots of average horizontal wavenumber and average horizontal position, respectively. It is seen that $\langle k_x \rangle$, $\langle k_y \rangle$, and $\langle y \rangle$ fluctuate about their initial values, with no significant net change. $\langle x \rangle$ increases approximately linearly with time, the packet moving with an average horizontal speed of less than 1 km per day. (For comparison, an average Garrett–Munk wave group travels 11 km in a day.) In the eikonal picture, therefore, horizontal transport is irrelevant.

Figure 4 shows a plot of average vertical wavenumber, $\langle k_v \rangle$, as a function of time. During the first half inertial period, there is a smooth six-fold increase in $\langle k_v \rangle$. (The corresponding decrease in wavelength is from $\langle \lambda_v \rangle \approx 130$ m to $\langle \lambda_v \rangle \approx 20$ m.) After this time, $\langle k_v \rangle$ fluctuates wildly. There are seen to be breaks in the $\langle k_v \rangle$ curve, shown by dotted lines. Each break

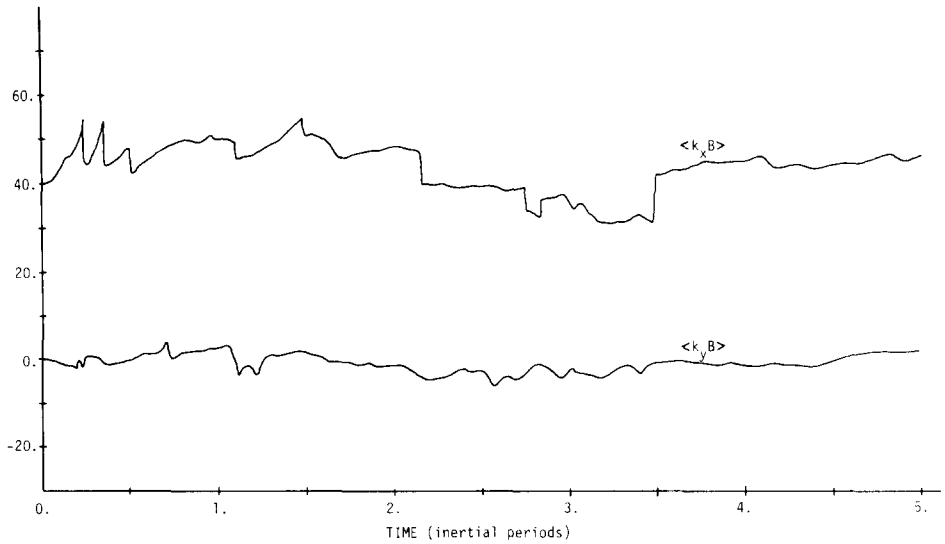

Fig. 2. Behavior in time of average horizontal wavenumber. The wavenumber components are non-dimensionalized using the Vaisala scale depth B = 1.3 km, the unit of time is one inertial period. Averages are over the ensemble of surviving trajectories, which numbers 50 at $t = 0$. $\langle k_x \rangle$ and $\langle k_y \rangle$ fluctuate about their initial values.

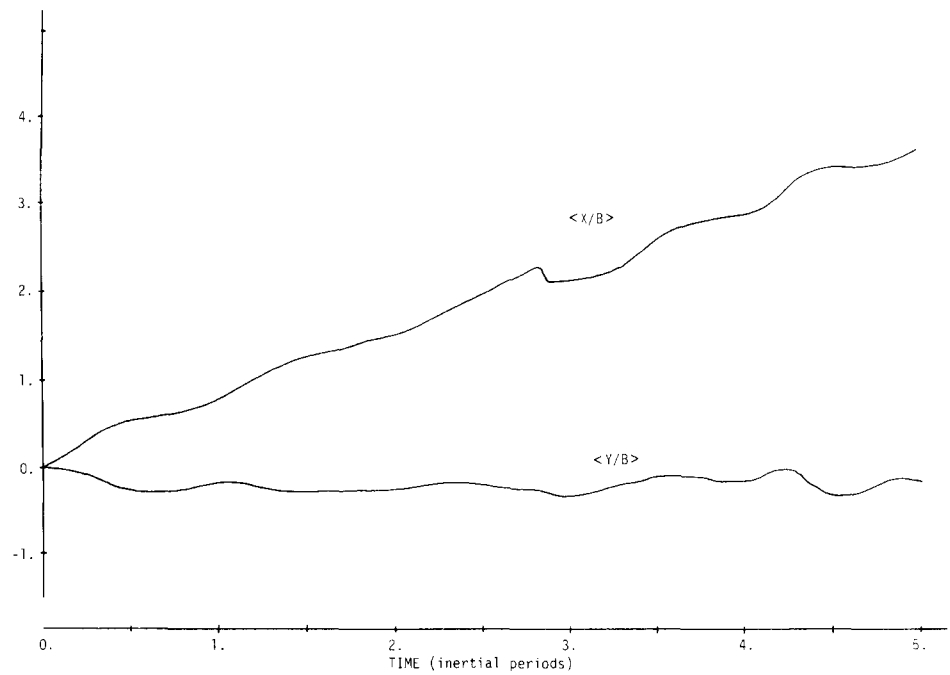

Fig. 3. Behavior in time of average horizontal position. $\langle x \rangle$ increases slowly whereas $\langle y \rangle$ fluctuates about zero. There is clearly a memory of the deterministic part of the initial velocity components.

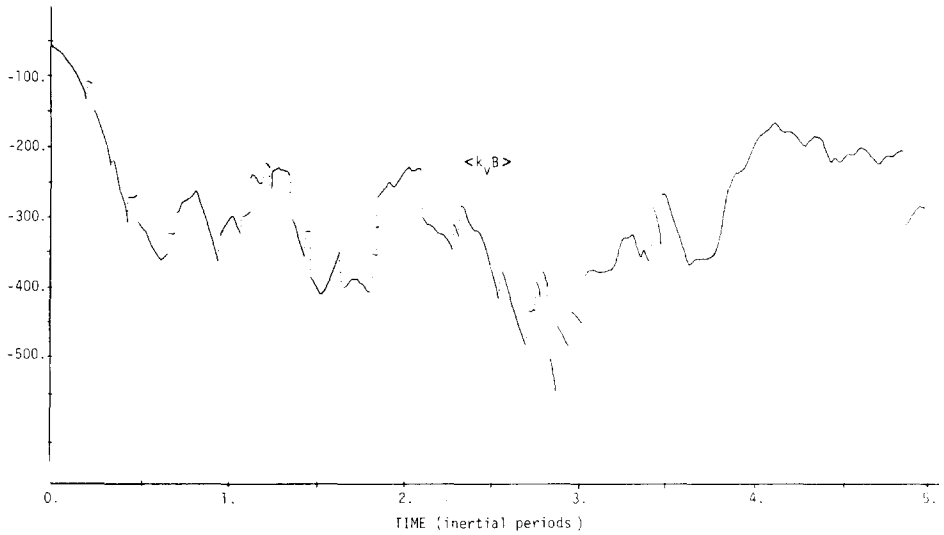

Fig. 4. Average vertical wavenumber as a function of time. Breaks in the curve correspond to "critical layer events" which occur when the value of $|k_v|$ along a trajectory exceeds the cut-off value ($2\pi/|k_v| = 5$ m is the equivalent wavelength).

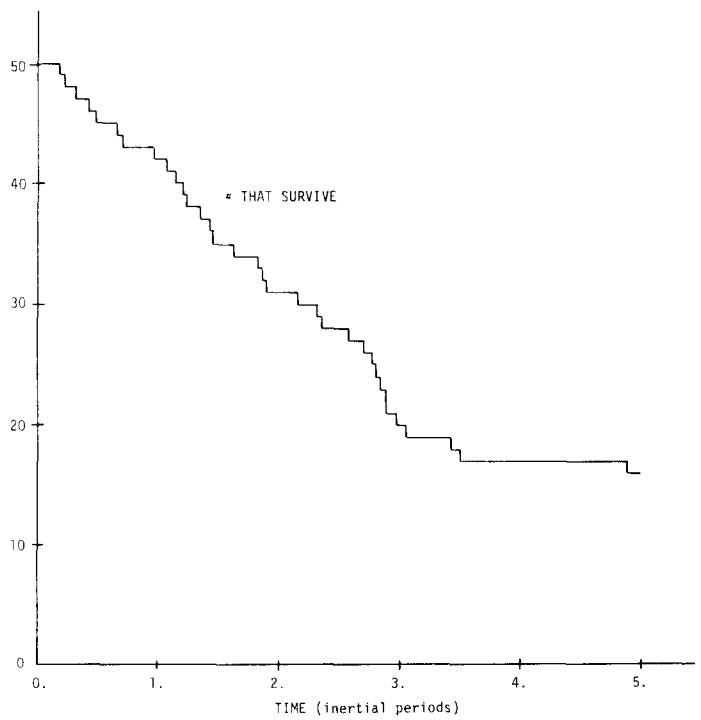

Fig. 5. The number of trajectories which have survived the cut-off criterion as a function of time. In five inertial periods, 34 out of 50 trajectories did not survive.

corresponds to a trajectory of the original 50-member ensemble which satisfies the $\lambda_v = 5$ m cut-off criterion. It is removed from the ensemble, and subsequent averages are taken over the surviving members. Since the trajectory being removed has a significantly higher (positive or negative) k_v value than the average, we see a discontinuity in the $\langle k_v \rangle$ curve. Out of the original 50 members of the ensemble, 34 encountered a "critical layer" during the five inertial periods. Figure 5 shows a histogram plot of the number of surviving trajectories versus time. After the first critical layer event, the number of survivors decreases at an approximately constant rate. Eventually, a set of trajectories remain which show little inclination toward reaching a critical layer. (This behavior was typical of a number of wave packet initial conditions we tried.) Twentyfive of the 34 trajectories which reached a critical layer did so with a negative k_v value, i.e., traveling in the same vertical direction as at $t = 0$; individual trajectories tend to preserve their direction in spite of large changes in their vertical wavenumber caused by the ambient shear.

In Fig. 6 we show plots of $k_v(t)$ for three individual trajectories. The solid curve satisfies the $\lambda_v < 5$ m cut-off after less than one inertial period, reaching the cut-off with a positive k_v value (i.e., this trajectory did change direction). The dashed curve represents a trajectory which survived for three inertial periods. During the first two of these periods the magnitude of k_v

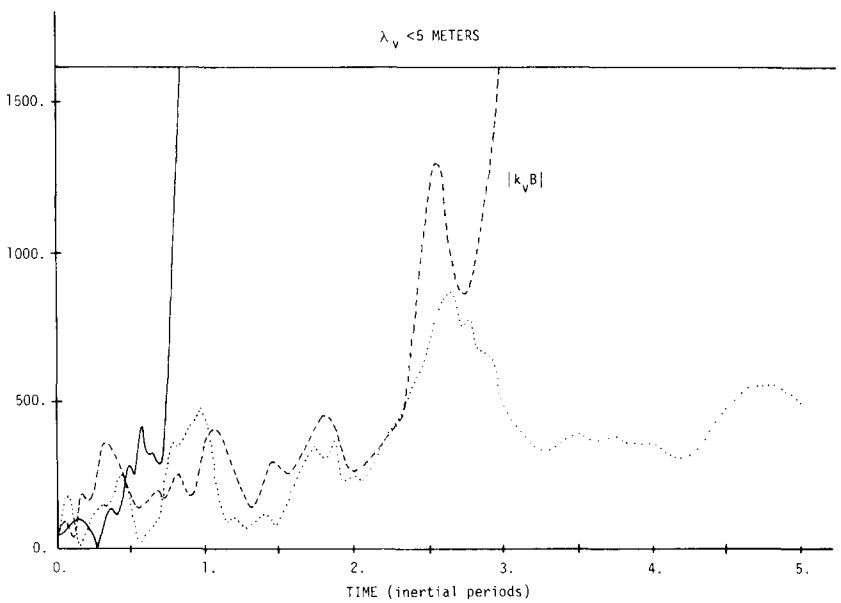

Fig. 6. Vertical wavenumbers as a function of time for three individual members of the ensemble of trajectories. Two of the three trajectories shown here reach a "critical layer".

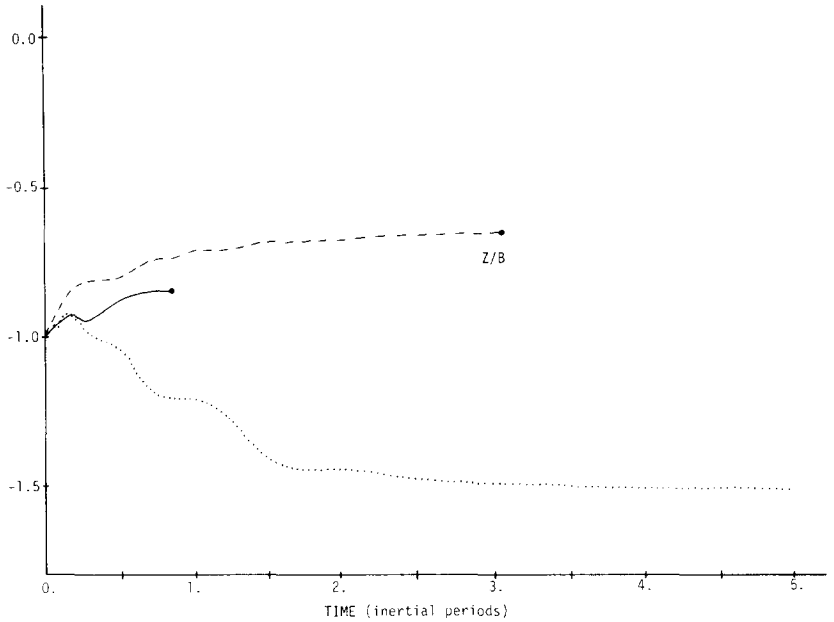

Fig. 7. Depth as a function of time for the same three trajectories as in Fig. 6.

increased (with fluctuations) to $|k_v B| \approx 300$. Subsequently, there was a rapid four-fold increase in magnitude, followed by a short-lived decrease, then a final surge through the cut-off. The third trajectory, shown in Fig. 6 as dots, survived the full course of five inertial periods and shows a net increase in vertical wavenumber to about $|k_v B| \approx 300$. Figure 7 shows wave packet depth, $z(t)$, for the same trajectories as in Fig. 6. Since $\dot{z} = \partial_{k_v} \sigma$ becomes

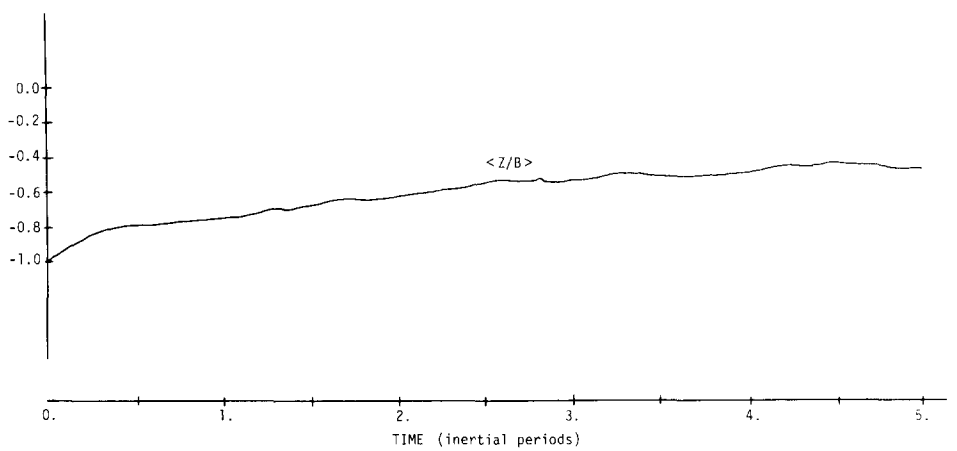

Fig. 8. Average depth versus time for the full ensemble of trajectories. Rapid changes in z can only occur when the vertical wavenumber is small.

small when $|k_v|$ is large (as do $\dot{x}$ and $\dot{y}$), the wave packet comes to a near halt as a critical layer is approached. This can be seen in the figure.

Returning to ensemble average quantities, Fig. 8 shows the time dependence of average depth. We see little vertical motion after the first quarter inertial period due to the occurrence of critical layers. Finally, Figs. 9 and 10 show average intrinsic frequency, $\langle \sigma \rangle$, and average total frequency, $\langle \omega \rangle$, as functions of time. The decrease in $\langle \sigma \rangle$ is tied to the increase in $\langle |k_v| \rangle$. Raggedness of the curves is due to the limited size of the ensemble. Both figures (especially Fig. 10) show an envelope oscillation with a period of approximately 1 day (also see $\langle k_v \rangle$ plot). The reason for this is the selection of background wavenumbers and frequencies from the Garrett–Munk spectrum: the spectrum strongly weights frequencies toward inertial values.

From our numerical results we see that the dominant transport is in the vertical wavenumber, k_v. This transport is shared between a mean motion of k_v to large values, with the same sign as at $t = 0$, and fluctuations about that mean. The individual excursions in k_v are of large magnitude. The existence of a large mean motion, and the size of the individual excursions, both show

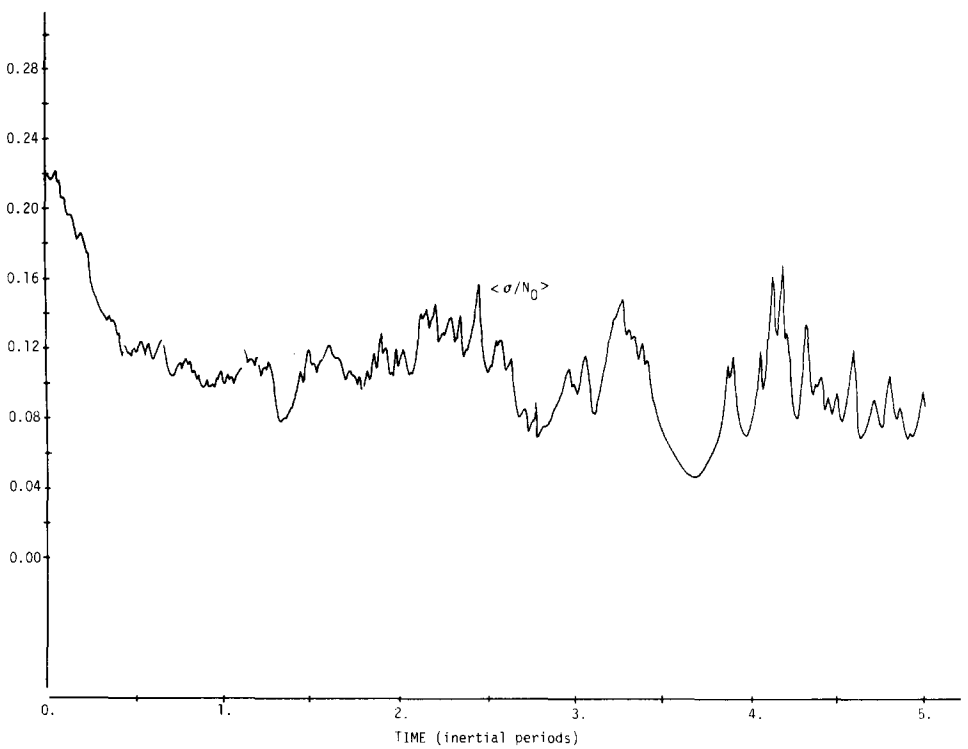

Fig. 9. Intrinsic frequency (scaled by the surface Vaisala frequency $N_0 = 3$ c.p.h.) as a function of time.

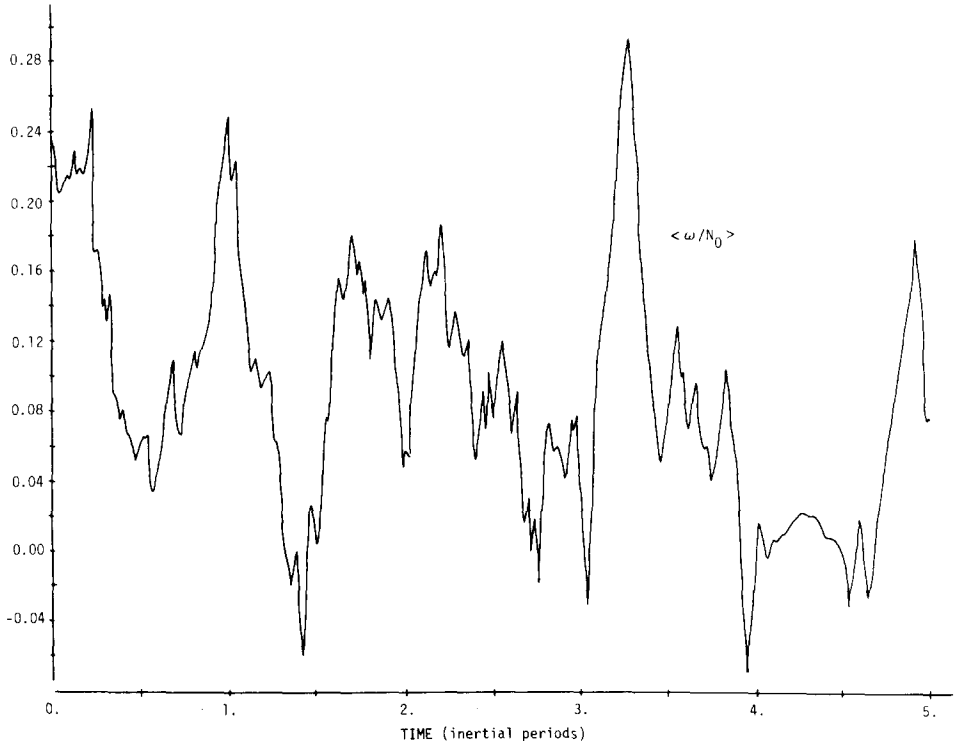

Fig. 10. Total (Doppler shifted) frequency as a function of time. Since σ becomes small at high vertical wavenumber, the behavior of ω is dominated by $\mathbf{u}\cdot\mathbf{k}_h$. An envelope oscillation with an approximate period of one day is seen because the G.M. frequency spectrum of background waves is strongly weighted to the inertial end.

the idea of diffusion in k_v–t space, implying a random walk, is inappropriate.

The large value of the mean motion of k_v leads us to a qualitative picture of the dominant transfer mechanism. The evolution of k_v is determined by

$$\dot{k}_v = -\partial_z \mathbf{u}\cdot\mathbf{k}_h \tag{73}$$

(neglecting a much more gentle z-dependence in N^2) so that

$$\langle \dot{k}_v \rangle = -\langle \partial_z \mathbf{u}\cdot\mathbf{k}_h \rangle \approx -\langle \partial_z \mathbf{u}\rangle \cdot \mathbf{k}_h \tag{74}$$

since $\mathbf{k}_h$ does not seem to have significant transport. Thus, mean motion of k_v requires nonvanishing $\langle \partial_z \mathbf{u}\rangle$. The quantity $\partial_z \mathbf{u}$, however, is a random function of space and time, primarily of the vertical position of the wave packet.

In order to explain how $\langle \partial_z \mathbf{u}\rangle$ arises, we imagine that at an initial time, $\langle \partial_z \mathbf{u}\rangle = 0$. The wave packet may find itself in either a shear which increases

the magnitude of k_v or a shear which decreases the magnitude of k_v, with equal probability. If $|k_v|$ starts to increase, the wave packet will slow down, since its vertical speed is approximately Nk_h/k_v^2. Then it is likely to remain in a shear of the same sign, and $|k_v|$ continues to increase. If, on the other hand, $|k_v|$ begins to decrease, the speed increases, and the packet moves to another depth at which the sign of the shear is uncorrelated with the initial shear. Thus, on the average, the packet seeks out a shear with the sign to make $|k_v|$ increase, leading to a mean motion of k_v. When k_v gets large enough, the wave packet finds itself approaching a critical layer. Only a change in sign of the shear caused by the time dependence of the background can cause k_v to start decreasing. If this change of shear does not happen soon enough, the wavelength of the packet gets extremely small, and presumably dissipation processes occur which destroy the wave packet. The numerical results indicate that an estimate of the rate at which $|k_v|$ increases from its mean level to the cut-off (see Fig. 6) is that the rate is one to two times $Nk_h/(2\mathrm{Ri})^{1/2}$, where Ri is the background Richardson number of order (1). Thus, the wave packet selects the sign of the shear, and positions itself in a place where the magnitude of the shear is slightly larger than the r.m.s. value.

Our picture of the transport suggests a simple statistical model which describes much of the transport that occurs. Consistent with the numerical results, this model ignores the time dependence and horizontal space dependence of the background. If we also ignore the reflections of trajectories at the surface and at turning points where $\sigma = N(z)$ (this was true of about 50% of our trajectories), some interesting deductions can be made.

The simple model has the property that vertical propagation is monatonic. As a result, the vertical position, z, can replace time as the independent variable. Since ω is independent of time, we can write

$$\frac{\partial \sigma}{\partial z} = -\partial_z \mathbf{u} \cdot \mathbf{k}_h \equiv G(z) \tag{75}$$

We imagine an ensemble of trajectories, starting at a given $z = z_0$ and having a given value of the intrinsic frequency, $\sigma = \sigma_0$, but different background realizations (just as with our numerical runs). Equation 75 is a stochastic differential equation for σ, driven by a Gaussian shearing force $G(z)$ with a correlation length ($\simeq 10$ m) short compared with the scale of variation of σ. By analogy with the theory of Brownian motion (e.g. Feller, 1966), the statistical properties of σ can be obtained from a diffusion equation for the probability density, $P(z, \sigma)$:

$$\frac{\partial P(z, \sigma)}{\partial z} = D \frac{\partial^2 P(z, \sigma)}{\partial \sigma^2} \tag{76}$$

D is the diffusivity, defined as

$$D = \int \langle G(z')G^*(0)\rangle \mathrm{d}z' \tag{77}$$

$$\approx \frac{k_h^2}{2} \times \text{shear spectrum evaluated at } k_v \approx 0$$

For the GM-79 spectrum, D has the value

$$D = 1.7\, k_h^2 (N/N_0)^2 \text{ (c.p.h.)}^2 \text{ m} \tag{78}$$

In order to obtain the finite value in (78), we have neglected the vanishing of the shear spectrum at low k_v by setting $m^2/(m^2 + 9)$ equal to unity.

The presence of critical layers provides eq. 76 with an absorbing boundary condition

$$P(z, f) = 0 \tag{79}$$

The solution of (76) with (79) is (see Feller, 1966, p.328)

$$P(z, \sigma) = \left(4\pi \left| \int_{z_0}^{z} D(z')\mathrm{d}z' \right| \right)^{-1/2} \left\{ \exp\left[-(\sigma - \sigma_0)^2/4 \left| \int_{z_0}^{z} D(z')\mathrm{d}z' \right| \right] \right.$$
$$\left. - \exp\left[-(\sigma + \sigma_0 - 2f)^2/4 \left| \int_{z_0}^{z} D(z')\mathrm{d}z' \right| \right] \right\} \tag{80}$$

(A more complete calculation would have included an absorbing barrier at $\sigma = N$ to take care of the turning point.)

The density of critical layers can be determined by differentiating the normalization $\int \mathrm{d}\sigma P(z, \sigma)$ with respect to z. This obtains

$$\rho = \left(L/\pi |z - z_0|^3 \right)^{1/2} \mathrm{e}^{-L/|z - z_0|} \tag{81}$$

where

$$L = (\sigma_0 - f)^2/4D \tag{82}$$

has the dimensions of length. The most probable value of ρ occurs at $|z - z_0| = 2L/3 \simeq 260$ m for the initial conditions used in our numerical experiments, and the distribution has a long tail whose meaning is irrelevant since our assumptions break down there. There appears to be no easy way of obtaining statistical information about the time dependence of critical layer events.

If our picture of the transport is correct, then all previous calculations have made an invalid approximation for computing the transport of action through vertical wavenumber space. Traditional calculations, in addition to assuming the interaction is weak, have also assumed that the motion during a correlation time of the background is essentially independent of the

background. Thus, the group velocity of the packet is considered constant (aside from its dependence on a variable Brunt–Vaisala frequency) in calculating the transport. Even the Taylor–Goldstein calculation of Meiss and Watson (which avoided the weak interaction assumption) needed an assumption equivalent to the requirement that the group velocity does not respond to the background, in order to convert their formal solution (a time ordered exponential of an integral) into an actual solution. Our picture requires the position of the test wave to be strongly correlated with the background, so that k_v is usually positive. The initial position is taken to be uncorrelated with the background, so this correlation arises through $\int_0^t \mathrm{d}t\, \mathbf{v}_{\mathrm{group}}(t)$ which requires dependence of $\mathbf{v}_{\mathrm{group}}$ on the background. Thus, the approximation schemes of all previous calculations are inconsistent with our picture of the dominant transport. Furthermore, we have argued that induced diffusion describes diffusion in σ–z space, not in k_v–t space as previously believed.

Since the completion of this work we have explored in detail the connection of our picture of transport with previous calculations. Confirmation of much of what we speculate in the above paragraph forms the content of a paper in preparation.

ACKNOWLEDGEMENT

Financial support was provided by independent reasearch funds of the La Jolla Institute.

REFERENCES

Feller, W., 1966. An Introduction to Probability Theory and its Applications, Volume II. Wiley, New York, pp. 328–329.

Garrett, C.J.R., 1967. Discussion: the adiabatic invariant for wave propagation in a non-uniform moving medium. Proc. R. Soc. London, Ser. A, 299: 26–27.

Garrett, C.J.R. and Munk, W.H., 1979. Internal waves in the ocean. Annu. Rev. Fluid Mech., 11: 339–369.

Gregg, M.C., 1977. A comparison of finestructure spectra from the main thermocline. J. Phys. Oceanogr., 7: 33–40.

Hasselman, K., 1962. On the non-linear energy transfer in a gravity-wave spectrum. J. Fluid Mech., 12: 481–500.

Henyey, F.S., 1980. Improved ray description of wave equations. Phys. Rev. Lett., 45: 1897–1900.

Henyey, F.S., 1981. Hamiltonian description of stratified fluid dynamics. Phys. Fluids, 26: 40–47.

Holloway, G., 1982. On interaction time scales of oceanic internal waves. J. Phys. Oceanogr., 12: 293–296.

Landau, L.D., and Lifshitz, E.M., 1975. The Classical Theory of Fields. 4th rev. Engl. edn., Pergamon Press, Oxford, pp. 129–157.

McComas, C.H., 1977. Equilibrium mechanisms within the oceanic internal wave field. J. Phys. Oceanogr., 7: 836–845.

McComas, C.H. and Bretherton, F.B., 1977. Resonant interaction of oceanic internal waves. J. Geophys. Res., 82: 1397–1412.

McComas, C.H. and Muller, P., 1981. The dynamic balance of internal waves. J. Phys. Oceanogr., 11: 970–986.

McIntyre, M.E., 1981. On the "wave-momentum" myth. J. Fluid Mech., 106: 331–347.

Meiss, J.D., and Watson, K.M., 1982. Internal wave interactions in the induced diffusion approximation. J. Fluid Mech., 117: 315–341.

Miles, J.W., 1977. On Hamilton's principle for surface waves. J. Fluid Mech., 83: 153–158.

Morrison, P.J. and Greene, J.M., 1980. Noncanonical Hamiltonian density formulation of hydrodynamics and ideal magneto-hydrodynamics. Phys. Rev. Lett., 45: 790–794.

Munk, W.H., 1981. Internal waves and small-scale processes. In: B.A. Warren and C. Wunsch (Editors), Evolution of Physical Oceanography. MIT Press, Cambridge, pp. 264–291.

Olbers, D.J., 1976. Nonlinear energy transfer and the energy balance of the internal wave field in the deep ocean. J. Fluid Mech., 74: 375–399.

Pomphrey, N., Meiss, J.D. and Watson, K.M., 1980. Description of nonlinear internal wave interactions using Langevin methods. J. Geophys. Res., 85: 1085–1094.

Seliger, R.L., and Whitham, G.B., 1968. Variational principles in continuum mechanics. Proc. R. Soc. London, Ser. A, 305: 1–25.

Shampine, L.F. and Gordon, M.K., 1975. Computer solution of ordinary differential equations: the initial value problem. Freeman, San Francisco.